ELSEVIER

Atmospheric Research 63 (2002) 39–58

ATMOSPHERIC RESEARCH

www.elsevier.com/locate/atmos

Tropospheric aerosol layers after a cold front passage in January 2000 as observed at several stations of the German Lidar Network

Ronald Eixmann [a,*], Christine Böckmann [b], Barbara Fay [c], Volker Matthias [d], Ina Mattis [e], Detlef Müller [e], Stephan Kreipl [f], Johannes Schneider [a,1], Andreas Stohl [g]

[a] *Leibniz-Institut für Atmosphärenphysik, D-18225 Kühlungsborn, Germany*
[b] *Institut für Mathematik Universität Potsdam, D-14469 Potsdam, Germany*
[c] *Deutscher Wetterdienst, D-63067 Offenbach, Germany*
[d] *Max-Planck-Institut für Meteorologie, D-20146 Hamburg, Germany*
[e] *Institut für Troposphärenforschung, D-04303 Leipzig, Germany*
[f] *Frauenhofer Institut für Atmosphärische Umweltforschung, D-82467 Garmisch-Partenkirchen, Germany*
[g] *Technische Universität München, Lehrstuhl für Bioklimatologie und Immissionsforschung, D-85354 Freising-Weihenstephan, Germany*

Received 10 July 2001; accepted 8 January 2002

Abstract

Using the German Lidar Network, we analysed 2 years of lidar observations of aerosol layers. Here we report in particular on a cold front event in January 2000 with Rayleigh/Mie/Raman lidar measurements taken both in the boundary layer as well as in the free troposphere at four different sites. After the cold front passage, and while the air mass travelled from northern to southern Germany, the aerosol backscatter coefficient increased in the lower troposphere but not in the free troposphere. Behind the front, an aerosol layer was observed in the free troposphere at all stations. To characterize changes in the aerosol layer as it moved from northern to southern Germany, backscatter profiles measured at Kühlungsborn and Hamburg were compared with profiles at Leipzig and Garmisch-Partenkirchen, respectively. This case study shows that an aerosol layer can persist in the free troposphere over a period of a few days. From calculated backward trajectories, we conclude that the air mass was lifted from the boundary layer, most likely 2–3 days before the cold front reached the lidar stations in Germany. We also compare the results of different trajectory models with respect to the origin of the aerosol layer. They indicate continental aerosols from the center of the

* Corresponding author.
E-mail address: eixmann@iap-kborn.de (R. Eixmann).
[1] Now at Max-Planck-Institut für Chemie, D-55020 Mainz, Germany.

PII: S0169-8095(02)00007-8

North American continent, which is consistent with particle size inversion results from the lidar backscatter data.

Keywords: Lidar; Aerosol optical properties; German Lidar Network

1. Introduction

The influence of aerosols on the global radiation budget is of great uncertainty, due in part to their relatively short lifetimes. In the past, only fixed aerosol parameters have been used as inputs in global models (e.g., Shettle and Fenn, 1976). In situ measurements compiled for the Global Aerosol Data Set (GADS) (Hess et al., 1998) have the disadvantage that each of them were obtained over very short time periods. For this reason, one of the objectives of the German Lidar Network project (Bösenberg et al., 1998) is to derive general characterizations of vertical and horizontal aerosol distributions in the troposphere over an extended time period. Additionally, the evolution of aerosols was to be investigated with special emphasis on the influence of cold front passages on the aerosol distribution. Measurements after cold front passages are of particular interest because in this case, an exchange of air masses occurs on a very short time scale.

Stations of the German Lidar Network are the Leibniz-Institute of Atmospheric Physics Kühlungsborn, the Max-Planck-Institute of Meteorology Hamburg, the Institute for Tropospheric Research Leipzig, the Institute of Atmospheric Environmental Research Garmisch-Partenkirchen and the University of Munich.

Table 1
Measurements obtained after the cold front passages at Kühlungsborn December 1997–January 2000

Date after cold front	Aerosol layer in the free troposphere (km)	Calculated β_{aer}
17.02.98	–	Yes
16.04.98	–	Yes
12.05.98	–	Yes
09.08.98	4	Yes
13.08.98	3.2	Yes
16.08.98	–	Yes
26.10.98	–	Yes
19.03.99	–	No
29.04.99	–	Yes
05.08.99	–	Yes
06.08.99	–	Yes
11.08.99	–	No
13.09.99	–	Yes
11.10.99	3.5	Yes
14.10.99	–	No
28.10.99	2.5	Yes
18.01.00	4.8	Yes

If no β_{aer} is shown, the weather conditions were too adverse to take measurements.

The German Lidar Network started its measurements on December 1, 1997. In the following 26 months, 17 cold front passages were measured over Kühlungsborn (Table 1). A cold front passage in January 2000 was the only one between December 1997 and January 2000 that passed overall five stations of the German Lidar Network from north to south. Also, since excellent meteorological conditions persisted for performing measurements at different stations in the same air mass, we chose this case to examine aerosol evolution during the frontal passage.

2. Instruments and observations

Technical details of the lidar systems of the German Lidar Network are described by Alpers et al. (1999) and Bösenberg et al. (2001). During the January 2000 cold front event, measurements were obtained of the aerosol backscatter coefficient (β_{aer}) at laser wavelengths between 351 and 1064 nm during daytime at four lidar stations. The lidars at Kühlungsborn and Leipzig had the possibility of Raman measurements after sunset, which allowed the experimental determination of aerosol extinction coefficients (α_{aer}). During daytime, it was not possible to measure independent α_{aer}, because of high solar background (Ansmann et al., 1990). Hence, for comparisons of lidar stations, only β_{aer} were calculated using the algorithm described by Fernald (1984) and Klett (1985). To apply this procedure, it is necessary to know the molecule number density of the atmosphere and the Rayleigh scattering coefficients. These were derived from local radiosonde measurements. If local radiosonde measurements were not available, radiosonde measurements from the DWD (German Weather Service) or the US Standard Atmosphere (U.S. Standard Atmosphere, 1976) were used. For the calculation of aerosol backscatter coefficients, an intercomparison of the algorithms to calculate β_{aer} used by the different lidar stations was performed within the German Lidar Network (Bösenberg et. al., 2001). The algorithm intercomparison showed that in general, the data evaluation schemes of the different groups work well (Bösenberg et al., 2001). The error in β_{aer} was determined from the statistical error of the return signal, from the fixing of the lidar ratio as an important source of error and the chosen reference value at an altitude where β_{aer} is near zero. In an ideal case, the aerosol backscatter coefficient is zero at this reference height. The reference height has to be defined for each lidar station and each measurement case individually. Especially at longer wavelengths, (e.g., 1064 nm), it is hard to find both an appropriate reference altitude and a reference value, which leads to increased uncertainty for these wavelengths.

The DWD provided daily backward trajectories to examine the sources of the observed air mass. The trajectories describe the horizontal and vertical movements of a mass point representing the center of gravity of the air parcel. The backward trajectories were computed using results from the Global Model GME, which is the global weather forecast model of the DWD (Kottmeier and Fay, 1998). The meteorological data are on a horizontal grid of 60×60 km and comprise 31 vertical levels. Usually, the uncertainty of the trajectories decreases with increasing wind speed. Trajectory quality strongly depends on the precision of the weather forecast model but also on the accuracy of the trajectory

model. Trajectory errors amount to about 10–20% of the horizontal travel distance of the trajectories (Stohl, 1998).

The cold front in January 2000 moved from northern to southern Germany, crossing the lidar stations Kühlungsborn and Hamburg on January 17 around noon, Leipzig during January 18, and reaching Garmisch-Partenkirchen on January 19 (Fig. 1). These four lidar network stations obtained measurements during this event. The trajectories calculated for Leipzig and Garmisch-Partenkirchen (Fig. 2a,b) passed over northern Germany at all tropospheric altitude levels, therefore allowing comparisons of lidar backscatter profiles of the same air mass. Fig. 2a shows that the air mass that passed over Leipzig likely crossed the lidar station at Kühlungsborn at almost all levels. Likewise, the air mass arriving at Garmisch-Partenkirchen probably passed over the lidar station at Hamburg (Fig. 2b).

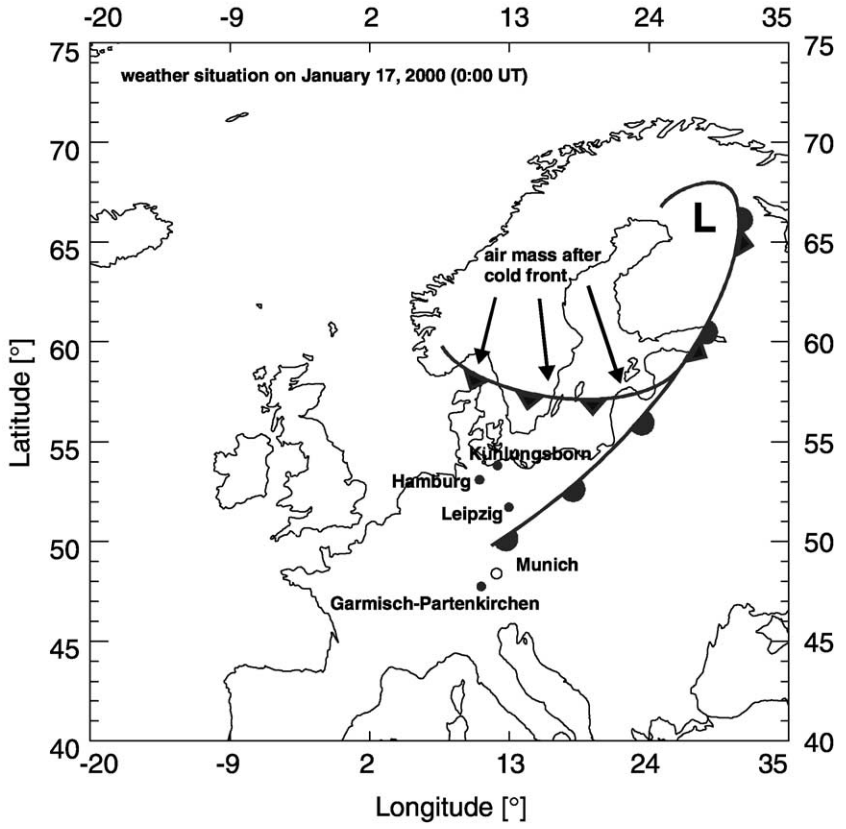

Fig. 1. Weather situation on January 17, 2000 at 00:00 UT. A cold front from northeastern Europe moved across the stations of the German Lidar Network in the following days. At Munich, the weather conditions where too bad to take measurements.

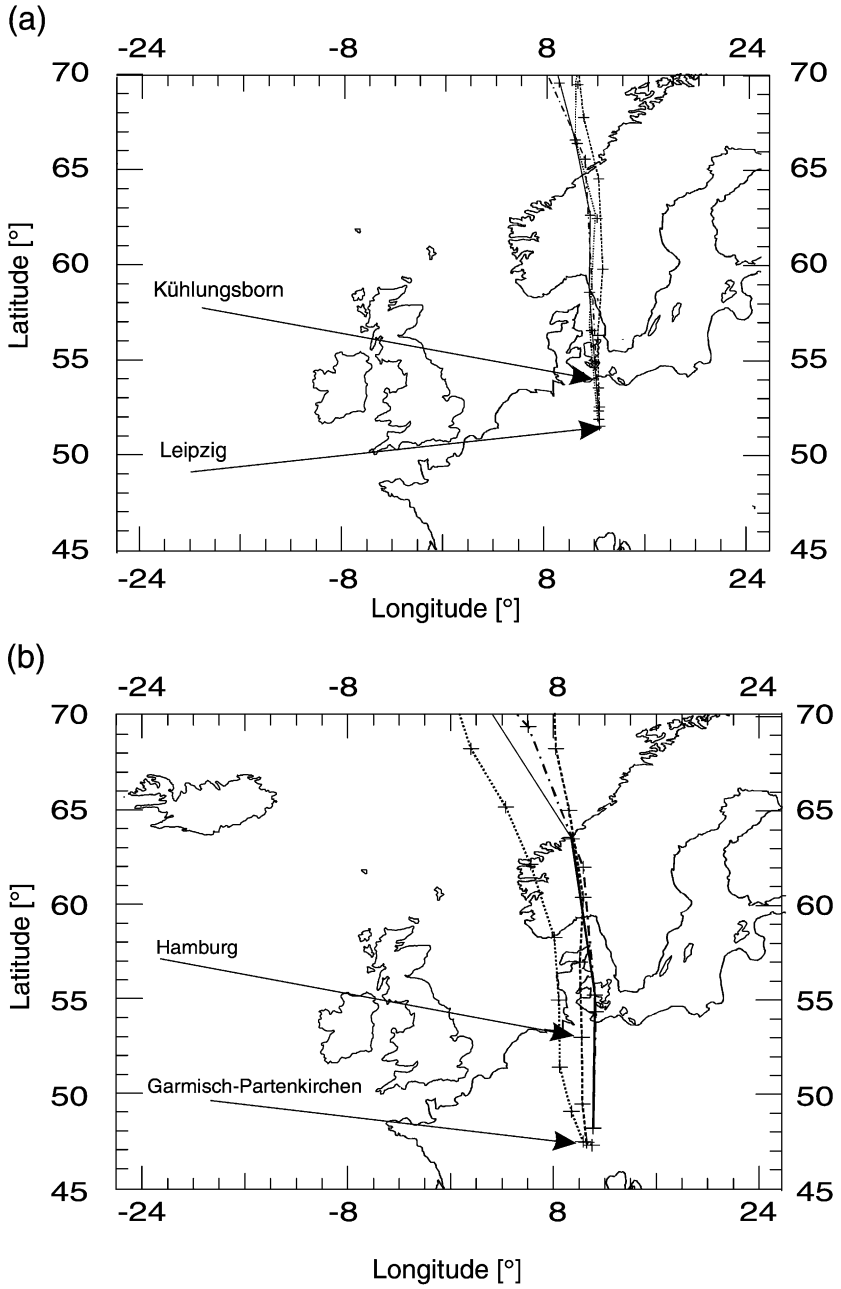

Fig. 2. (a) Backward trajectories (GME) arriving at Leipzig on January 18, 2000 at 13:00 UT. Dotted line, 850 h Pa; short dashed line, 700 h Pa; dash-dotted line, 500 h Pa; solid line, 300 h Pa. (b) Backward trajectories (GME) arriving at Garmisch-Partenkirchen on January 19, 2000 at 13:00 UT. Dotted line, 850 h Pa; short dashed line, 700 h Pa; dash-dotted line, 500 h Pa; solid line, 300 h Pa.

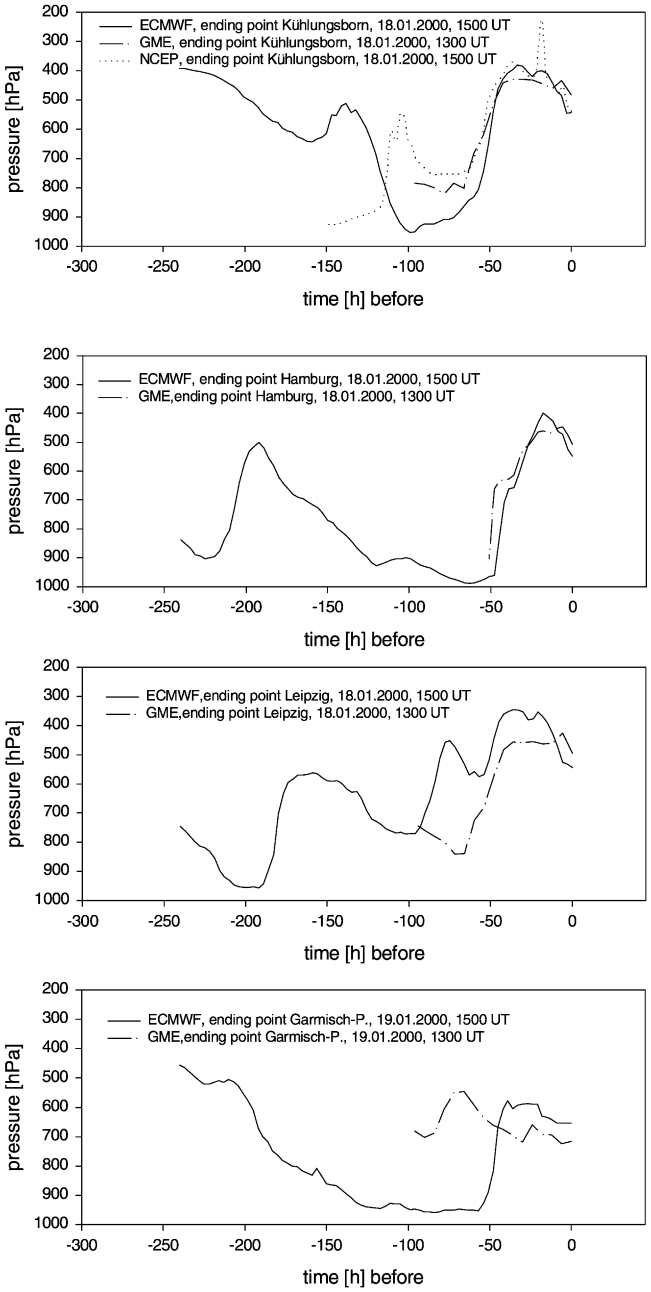

Fig. 3. Vertical evolution of the backward trajectories of the aerosol layer level arriving at Kühlungsborn, Hamburg, Leipzig and Garmisch-Partenkirchen on January 18–19, 2000 at 13:00 and 15:00 UT. Dashed line is the trajectory after GME (DWD), solid line is the trajectory after ECMWF and the dotted line is the trajectory after NCEP.

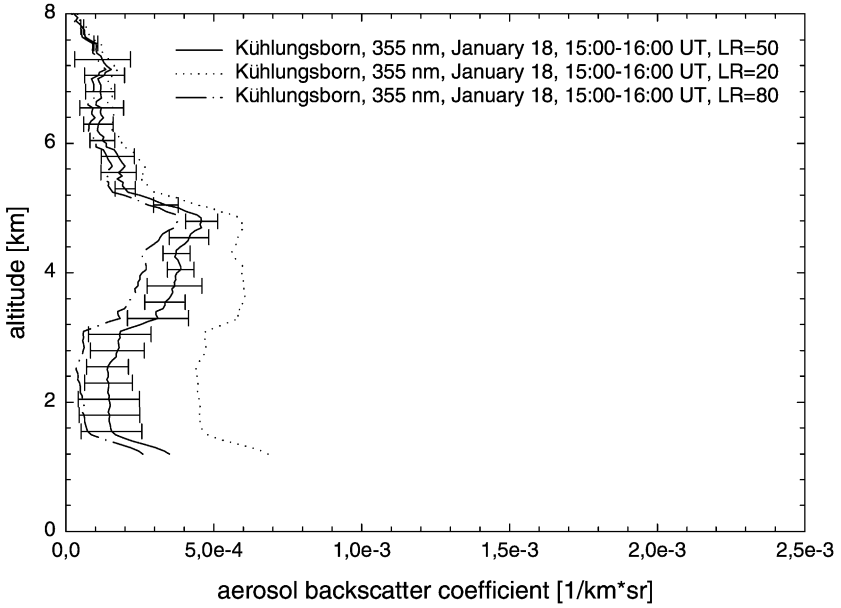

Fig. 4. Aerosol backscatter coefficients β_{aer} (Klett, 1985) for the wavelength 355 nm with different lidar ratios (S) for Kühlungsborn on January 18, 2000, 15:00–16:00 UT.

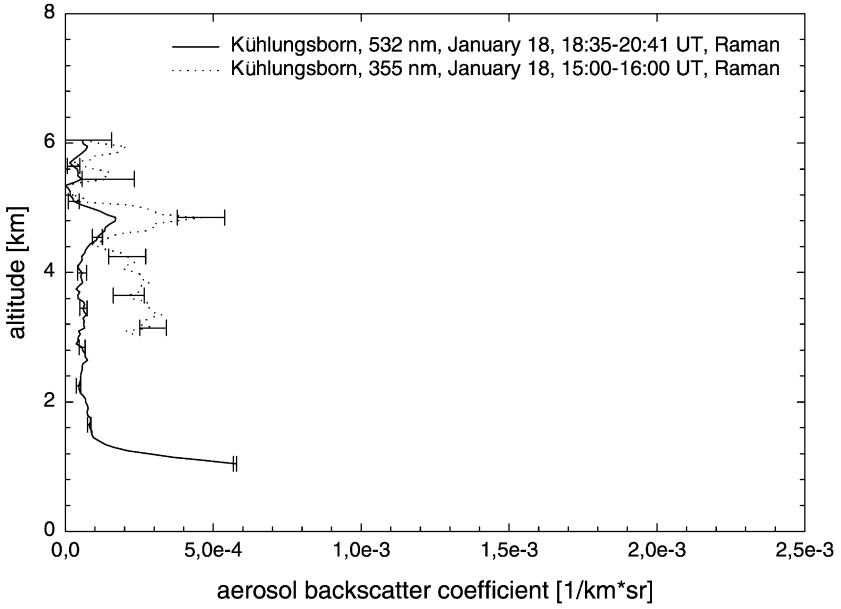

Fig. 5. Aerosol backscatter coefficients β_{aer} (Raman method) at the wavelengths 355 and 532 nm for Kühlungsborn on January 18, 2000, 15:00–16:00 UT.

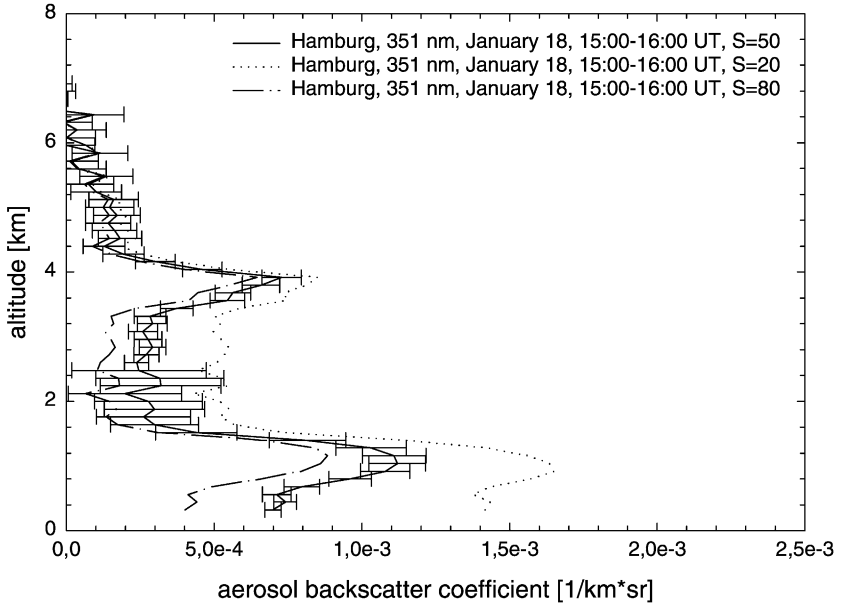

Fig. 6. Aerosol backscatter coefficients β_{aer} (Klett, 1985) at the wavelength 351 nm with different lidar ratios (S) for Hamburg on January 18, 2000, 15:00–16:00 UT.

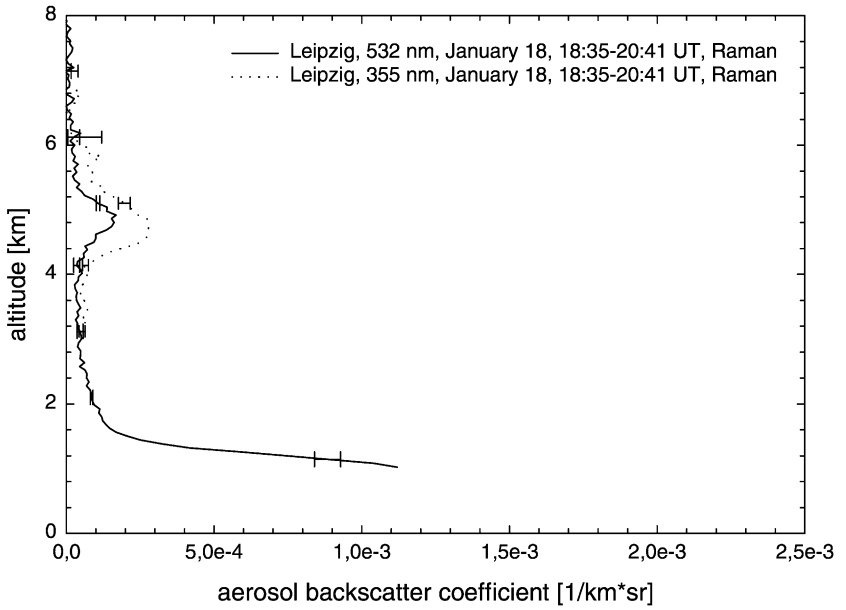

Fig. 7. Aerosol backscatter coefficients β_{aer} (Raman method) at the wavelengths 355 and 532 nm for Leipzig on January 18, 2000, 18:35–20:41 UT.

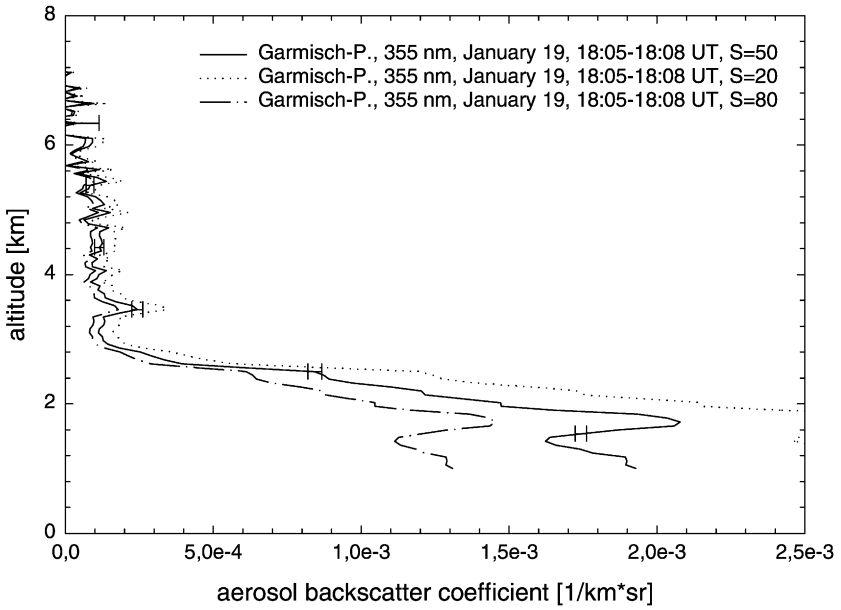

Fig. 8. Aerosol backscatter coefficients β_{aer} (Klett, 1985) at the wavelength 355 nm with different lidar ratios (S) for Garmisch-Partenkirchen on January 18, 2000, 18:05–18:08 UT.

Examining the vertical movement of the trajectories (Fig. 3), we see that they were lifted from near the boundary layer into the free troposphere 2 or 3 days before. β_{aer} measured at Kühlungsborn (355 nm) and Hamburg (at 351 nm) after the cold front passage on January 18 in the afternoon are illustrated in Figs. 4–6. The top of the boundary layer at Kühlungsborn was situated at 1.3 km a.s.l. (above sea level) and at Hamburg in 1.6 km a.s.l. The value of β_{aer} in the free troposphere is on average about 1.5×10^{-4} (km sr)$^{-1}$ at both locations. An aerosol layer was observed in the free troposphere over Kühlungsborn at 4.8 km a.s.l. and over Hamburg at 3.9 km a.s.l. About 5 h later, the air mass reached the lidar station Leipzig (Fig. 7) and 36 h later, it reached Garmisch-Partenkirchen (Fig. 8). Figs. 5 and 7 shows an increase in the boundary layer height by approximately 0.2 km over the distance of 300 km between Kühlungsborn and Leipzig. The altitude of the aerosol layer is approximately 4.8 km a.s.l. at both stations. In contrast to the eastern lidar stations, at the western stations, the aerosol layer descended 0.4 km while traveling from north to south. In Fig. 6, the aerosol layer over Hamburg is situated at 3.9 km a.s.l., while it was at 3.5 km a.s.l. in Garmisch-Partenkirchen (Fig. 8). Similar is the height of the planetary boundary layer (PBL), which is located at 1.6 km a.s.l. in Hamburg (situated at the river Elbe) and also at 1.6 km a.s.l. in Garmisch-Partenkirchen (situated in an alpine valley). However, the value of β_{aer} within the PBL at Garmisch-Partenkirchen (Fig. 8) is significantly larger than at Hamburg (Fig. 6), where the same air mass resided 36 h before.

Temperature, pressure and relative humidity obtained from a radiosonde launched at Schleswig (approximately 150 km northwest of Kühlungsborn) along with the backscatter

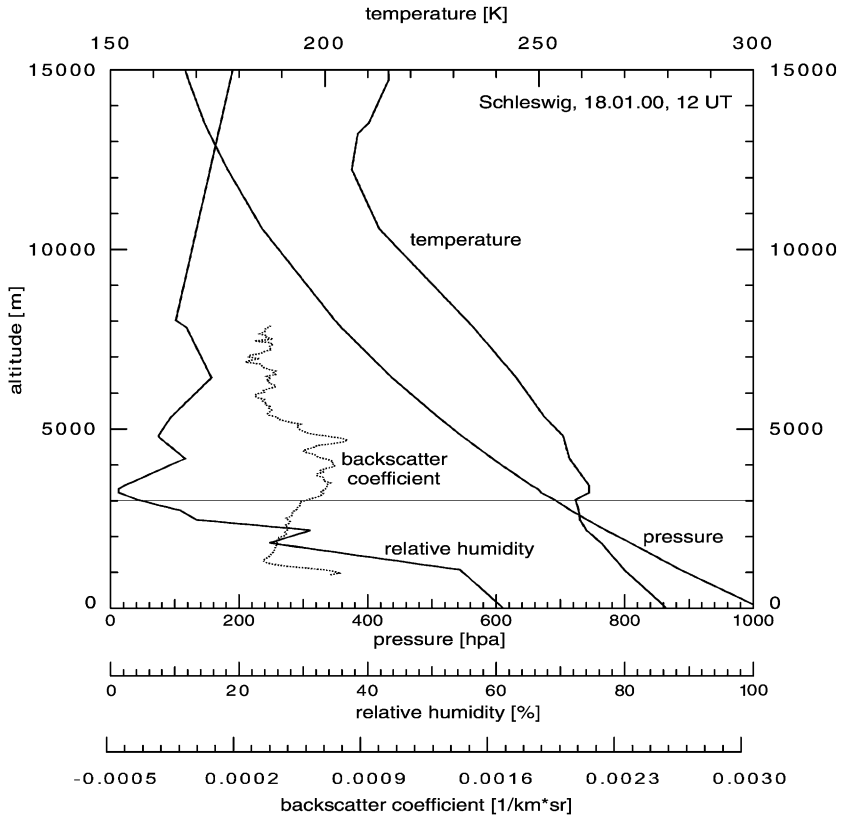

Fig. 9. Temperature, pressure and relative humidity obtained from a radiosonde launch at Schleswig (approximately 150 km northwest of Kühlungsborn), along with the backscatter profile measured at Kühlungsborn for the wavelength 355 nm on January 18. Between 3 and 5 km, the relative humidity is below 15%. The temperature profile shows an inversion at 3 km, limiting vertical exchange with the layers below.

profile are plotted in Fig. 9. The relative humidity was below 15% between 3 and 5 km height. The temperature profile shows an inversion at 3 km, which limited vertical air mass exchange to lower altitudes.

3. Discussion and results

3.1. Planetary boundary layer and free troposphere without an aerosol layer

The backscatter profiles at Kühlungsborn and Hamburg represent different measurements made at the same time (Figs. 4 and 6). The horizontal distance between these two stations is only about 150 km, but Kühlungsborn is situated in a rural environment close to the coastline of the Baltic Sea; Hamburg is situated in an urban environment not far away

from the North Sea. The backward trajectories calculated on the basis of GME of the DWD show that on January 18, the air masses above Kühlungsborn and Hamburg came from the north of Scandinavia, but the paths of the air masses from the source to the lidar stations were different. While the air mass at Kühlungsborn came from Scandinavia across the Baltic Sea, the air mass at Hamburg came from Scandinavia via Denmark. Comparison of the aerosol backscatter profiles from the two different air masses shows that the top of the PBL are similar in both cases.

A comparison of the backscatter profiles from all stations is possible because the time interval between the measurements corresponds to the time the air mass travelled from Kühlungsborn to Leipzig and from Hamburg to Garmisch-Partenkirchen, respectively. Weather charts confirm this facts. The comparison between Kühlungsborn (Fig. 5) and eipzig (Fig. 7) reveals that the PBL height did not change significantly over the distance of roughly 300 km. The PBL over Garmisch-Partenkirchen shows two maxima for the aerosol backscatter coefficient at the wavelength 355 nm, ones at 1.6 km and the other at 2.6 km. The PBL height of the second maxima at 2.6 km is 1.0 km above the PBL height in Hamburg. In contrast, the PBL height of the first maximum at 1.6 km is similar for both stations. The reason for the second maximum at 2.6 km at Garmisch-Partenkirchen was founded by local condensation of water vapor on this altitude level. The value of the β_{aer} in the PBL at Garmisch-Partenkirchen is twice than at Hamburg. The reason for the differences for β_{aer} in the PBL are most likely the 700 km distance between the two lidar stations. The air masses were loaded with urban and rural aerosol particles from the land surface transported into the atmosphere by friction and turbulence at the ground.

Comparisons of the aerosol backscatter coefficient in the free troposphere for both pairs of stations are shown in Figs. 6 and 8. The aerosol backscatter coefficients at Hamburg and Garmisch-Partenkirchen are nearly the same. The aerosol backscatter coefficient β_{aer} in the free troposphere is more than 10 times smaller than within the PBL without consideration of the aerosol layer in the free troposphere. Above the boundary layer, Rayleigh scattering is dominant at Hamburg and also at Garmisch-Partenkirchen. The comparison between the backscatter profiles from Kühlungsborn (Figs. 4 and 5) and Leipzig (Fig. 7) shows the same results. This showed that the changes of backscatter profiles were very small over a great distance.

3.2. Aerosol layer in the free troposphere

At all stations, the observed aerosol layer can be characterized by the following properties. It shows a downward slope from east to west since it was observed at Kühlungsborn and Leipzig at about 4.8 km, over Hamburg at 3.9 km and over Garmisch-Partenkirchen at 3.5 km. This slope was probably caused by the center of a high pressure system being located west of western Europe over the Atlantic Ocean. Therefore, subsidence during the anticyclonic movement of an air mass was much more pronounced at the western stations.

During the cold front event, the high pressure area moved from western to eastern Europe. For that reason, the aerosol layer descended 400 m from Hamburg to Garmisch-Partenkirchen. The pressure level of the aerosol layer over Kühlungsborn and Leipzig was

the same. These two lidar stations are further to the east than Hamburg and Garmisch-Partenkirchen, and their distance is only 300 km.

Data from a radiosonde launch at Schleswig (Fig. 9) reveal that the lower boundary of the aerosol layer at this location was in an altitude region with very low relative humidity (below 15%). Fig. 9 also shows a temperature inversion at the same level. The very low relative humidity and the temperature inversion are clear indicators of sinking air due to the high-pressure situation over Germany following the cold frontal passage. In a high-pressure area, the air descends adiabatically over a great area, leading to a temperature increase and a decrease of the relative humidity. The upper boundary of the PBL marks the lower boundary of the aerosol layer in the free troposphere. Therefore, vertical motions of the air mass and vertical mixing were prevented for an extended time period in the free troposphere. These meteorological conditions permit a long lifetime of an aerosol layer.

The vertical development of the backward trajectories after ECMWF (Fig. 3) shows that around 2–3 days prior to the measurements, the air mass was strongly lifted. The reason for this lifting was the prevalence of strong baroclinic conditions in this area at this time. During the vertical transport of aerosol particles from the boundary layer into the free troposphere, the aerosol properties could be changed through particle growth and probably cloud formation with increasing relative humidity. For this aerosol layer (and also for many other aerosol layers observed during 2 years of measurements), slow sinking of the air mass, which usually took place in high-pressure areas, was observed. During this sinking process, the aerosol particles dry out. After upward and subsequent downward movement, the aerosol layer contains particles with new chemical and physical properties. Therefore, the properties of the aerosol particles as derived from lidar measurements are difficult in identifying the source of the aerosol layer.

The GME backward trajectory model (DWD) shows strong vertical motions to the north of the Scandinavian coast. It is remarkable that this aerosol layer remained distinct over a distance of several thousand kilometers, in spite of its small vertical extent. This may have been due to the temperature inversion (Fig. 9), which would have prevented the vertical mixing in this altitude range.

3.3. Comparison of different trajectory models

A trajectory model, driven with wind fields of the GME (DWD) (Kottmeier and Fay, 1998), was used within the German Lidar Network. For comparison purposes, the trajectory model driven with wind fields from the ECMWF (Stohl et al., 1995) was also used. The results of this comparison are shown in Figs. 3 and 10a–d. The vertical progression in both cases suggests that the air mass was lifted from the boundary layer into the free troposphere 2–3 days before its arrival in Germany. However, a comparison of the geographical location where the air mass was lifted shows considerable differences between the two models. For the DWD backward trajectories, the lifting was located to the north of the Scandinavian coast, whereas the ECMWF trajectories show it taking place over North America (for arrival at Kühlungsborn and Leipzig) and in the north of the Atlantic Ocean (for arrival at Hamburg and Garmisch-Partenkirchen). These differences could be due to different dynamics and physics of the weather forecast models

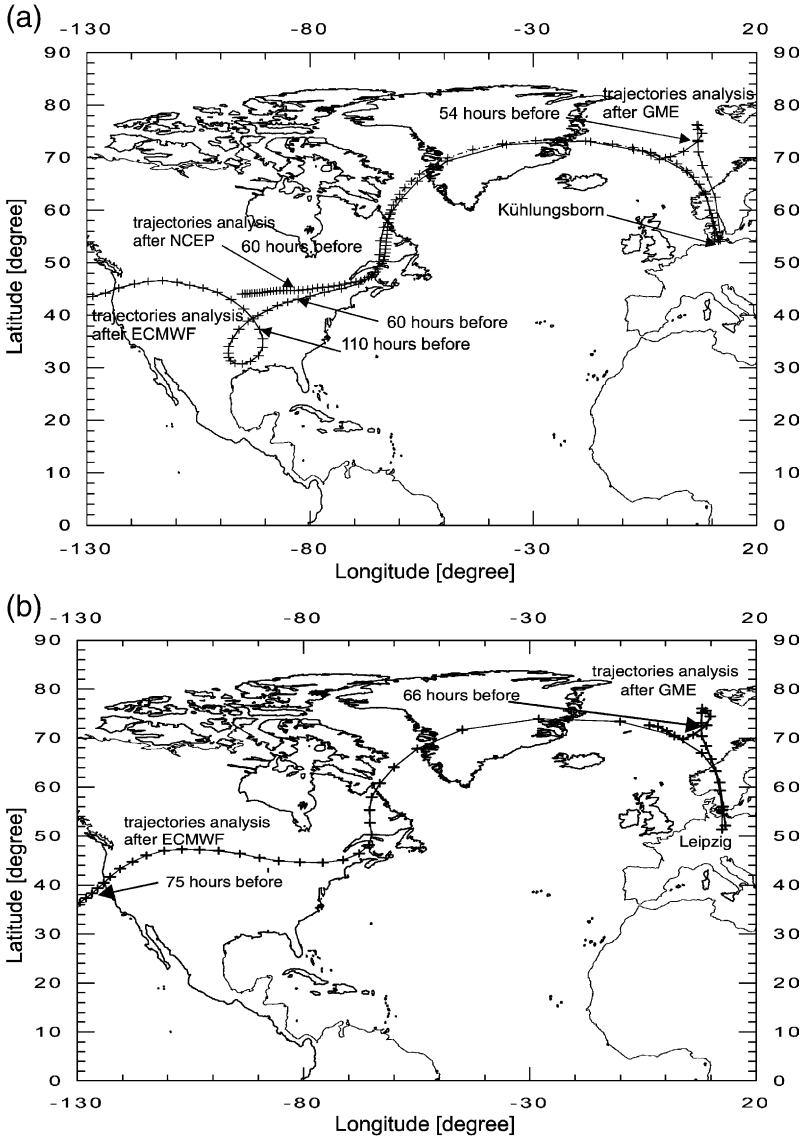

Fig. 10. (a) Backward trajectories for the three trajectory models GME, ECMWF and NCEP arriving at Kühlungsborn on January 18, 2000 at 13:00, 15:00 and 15:00 UT. (b) Backward trajectories for both trajectory models GME, ECMWF arriving at Leipzig on January 18, 2000 at 13:00 and 15:00 UT. (c) Backward trajectories for both trajectory models GME and ECMWF arriving at Hamburg on January 18, 2000 at 13:00 and 15:00 UT. (d) Backward trajectories for both trajectory models GME and ECMWF arriving at Garmisch-Partenkirchen on January 19, 2000 at 13:00 and 15:00 UT.

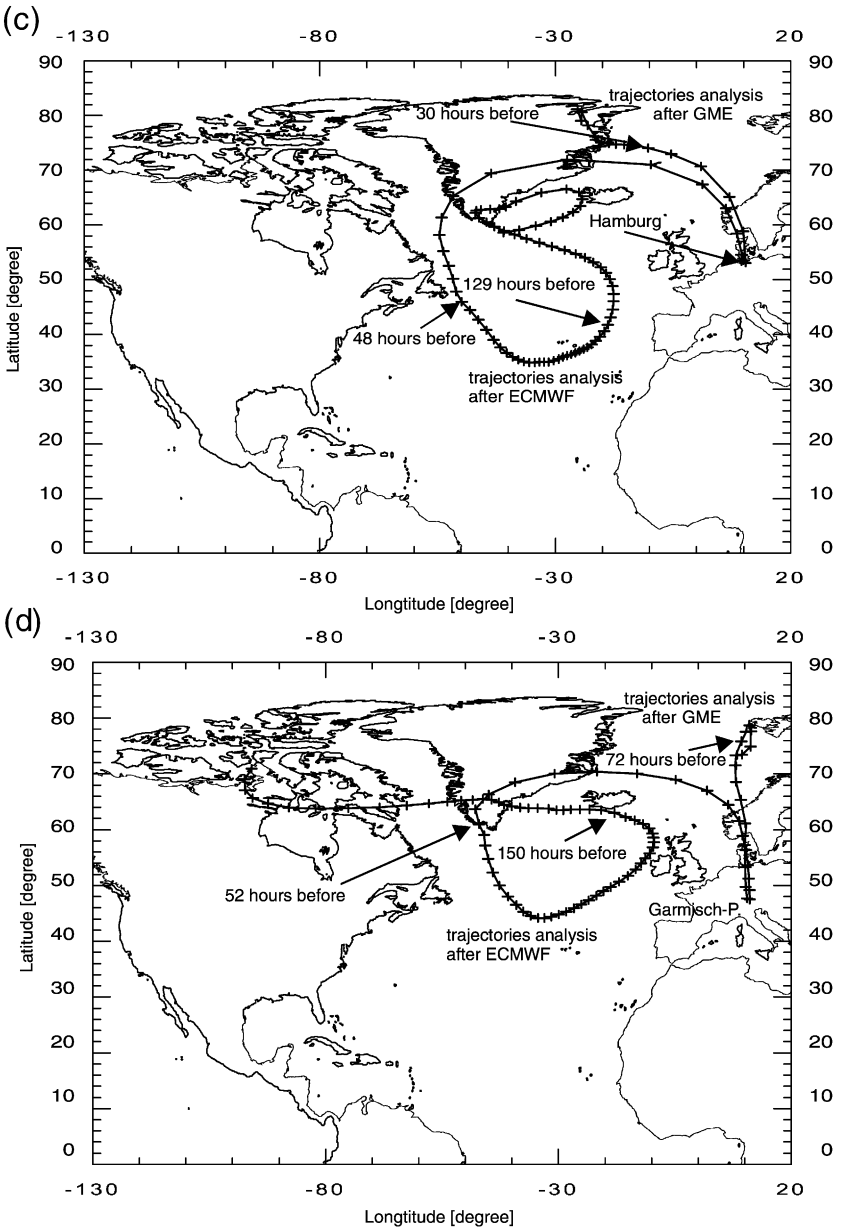

Fig. 10 (*continued*).

used to provide the input data, but they may also be due to different spatial and time resolution of the input data and to different trajectory model accuracy. Another possible reason is surely the fixed altitude levels for DWD-trajectories. They are only approxi-

mated to the altitude levels of the aerosol layer. In view of these results, another trajectory model was used, namely the HYSPLIT4[a] from NCEP[b] (HYSPLIT4, 1997). Results of this model are shown in Figs. 3 and 10a.

3.4. Calculation of particle properties

To derive additional properties of the observed aerosol layers, the spectral backscatter data provided by the Kühlungsborn lidar wavelengths were used to characterize the aerosol particles in this layer. The results for the derived values of β_{aer} are shown in Fig. 11, where the data are normalized to a wavelength of 532 nm. The error bars indicate the standard deviation, which is not existing at 532 nm due to the normalization. Also plotted in Fig. 11 is the wavelength dependence of β_{aer} for five different aerosol types, also normalized to 532 nm. These different aerosol types were taken from the software package Optical Properties of Aerosols and Clouds (OPAC), which is based on the Global Aerosol Data Set (GADS) and available on the World Wide Web (Hess et al., 1998). Typical aerosol components in this data set, such as sea salt, water soluble aerosol, and soot, are listed for low and high relative humidity. The aerosol backscatter coefficients of these aerosol types were compared with our measurements.

For the measured values in the aerosol layer, the standard deviation at a wavelength 355 nm is very large. Consequently, within this error bar, all aerosol components of the GADS data set are in agreement with our data. The 1064 nm coefficient from the measurement matches with the aerosol components "sea salt accumulation mode" at the lowest relative humidity (0%) and "water soluble" with large relative humidity (99%). However, Fig. 9 shows that at the altitude of the aerosol layer, the relative humidity was very low and thus the aerosol component "water soluble" should not have been applicable. In this way, it is possible to get at least a crude estimation for the particles in the aerosol layer, even though the results of lidar measurements for this thin aerosol layer are not very precise.

The physical properties of the particles were also derived by the inversion of optical data. For this purpose, an inversion scheme on the basis of Tikhonov's inversion with regularization (Tikhonov and Arsenin, 1977) was used that was designed for the retrieval of effective radius, volume, surface-area and number concentration, and wavelength-independent complex refractive index of the investigated particle size distributions (Müller et al., 1999a,b) from six-wavelength lidar observations (Althausen et al., 2000). A reduced data set of backscatter and extinction coefficients at the above-mentioned three wavelengths may be sufficient for the retrieval of the physical particle properties (Böckmann, 2001; Müller et al., in press).

The inversion is done by means of the numerical solution of the equations that relate the optical data to the microphysical particle properties. The particle parameters follow from approximations of volume concentration distributions, which are retrieved from the input optical data by means of linear combinations of B-spline functions of the first kind, i.e.,

[a] HYbrid Single-Particle Lagrangian Integrated Trajectory.
[b] The National Centers for Environmental Prediction, USA.

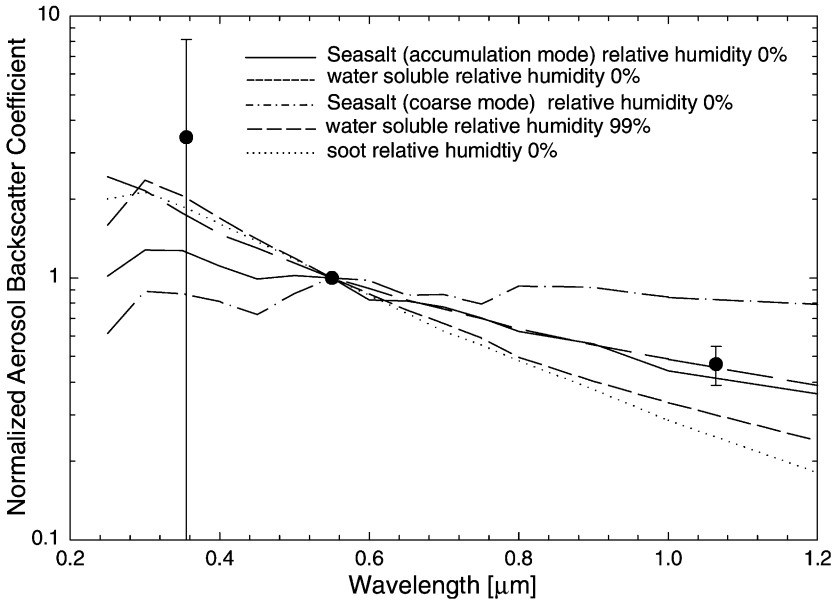

Fig. 11. β_{aer} in the observed aerosol layer normalized at the wavelength 532 nm, along with selected aerosol components from the Global Aerosol Data Set (GADS).

they have triangular shape on a semilogarithmic scale. Consequently, the inversion works independently of the shape of the particle size distributions.

The inversion is known to be a ill-posed problem, i.e., it is highly unstable. Small errors in the optical data lead to very large uncertainties, and the derived solution-space is not unique. In this procedure, a statistical analysis of the involved eigenvalues is done. Only those eigenvalues and respective eigenvector are used, which provide a good reconstruction of the investigated particle size distribution but at the same time suppress the error magnification. This so-called regularization is done by means of generalized cross-validation (Craven and Wahba, 1979; Golub et al., 1979). The introduction of B-splines in the first step and the introduction of additional constraints, e.g., smoothness and positivity of the derived particle size distributions further stabilizes the inversion.

For high-quality results, the errors in the optical data must be less than 20%. The nighttime measurements with the Raman-lidar at Leipzig were used for the inversion as this instrument allowed retrieval of the optical data with the necessary accuracy. For the inversion, the complete set of extinction coefficients at 355 and 532 nm and backscatter coefficients at 355, 532 and 1064 nm were used. Inversions were done for optical data sets in different height ranges within the layer, which extended from approximately 4.2 to 5.2 km. A detailed analysis of the optical profiles showed a two-layered structure within the particle layer. Particle extinction-to-backscatter ratio at 532 nm showed extremely high values of 100–140 sr from 4.3 to 4.7 km height, and decreased to 50–70 sr from 4.7 to 5.0 km in height. The differences suggest considerably different particle properties within the particle layer.

Because of relative large uncertainties of the optical data in the lower portion of the particle layer, reasonable inversion results could not be found. Within the center of the upper portion of the particle layer at 4.9 km height, the derived effective radius was 0.15 ± 0.01 μm (Table 2). The volume concentration was 2.5 ± 0.6 μm^3 cm^{-3} and the surface-area concentration was $49.8 \pm 8.6 \mu m^2$ cm^{-3}. The real part of the complex refractive index was 1.4 ± 0.05. For the imaginary part, a value of 0.004 ± 0.004 was found. A complex refractive index of $1.4-0.004i$ is consistent with values found for sea salt particles (d'Almeida et al., 1991; Hess et al., 1998). This finding is supported by the results from the DWD backward trajectories, which indicated the uplifting of airmasses above the Atlantic Ocean 3 days prior to the lidar observations. However, the large lidar ratio strongly contradicts the assumption of sea-salt particles. Theoretical studies (Ackermann et al., 1998) as well as measurements within the marine boundary layer (Ansmann, 2001) have shown lidar ratios of 20–25 sr for marine particles.

A better interpretation follows from the results of the ECMWF backward trajectories, which indicated the uplifting of airmasses above the North American continent a few days before the lidar observation. Given the large uncertainty in the derived imaginary part of the refractive index, values of up to $0.02i$ might indicate the presence of particles from urban-industrial sources. This is consistent with the observed high lidar ratios of 50–70 sr, which are characteristic of continental-polluted particles (Ansmann et al., 2001). Observations of industrial-pollution plume advected from the North American continent out over the Atlantic Ocean during the Tropospheric Aerosol Radiative Forcing Observational Experiment (Russel et al., 1999) showed imaginary parts of the refractive index below $0.017i$ in the visible wavelength range. These observations were made in spring time. Since combustion processes, for example for domestic heating, are more intense during winter, this might explain the observed higher imaginary part in our study. The real part of the refractive index of 1.4 found in the present study is at the lower end of the values found in TARFOX, which averaged 1.53 at relative humidities significantly above those found for this study.

A second inversion scheme, developed at the University of Potsdam in the Institute of Mathematics (UPM), was also used to retrieve microphysical particle properties

Table 2
Results of the inversion schemes after the University of Potsdam, Institute for Mathematics (UPM) and Institute for Tropospheric Research, Leipzig (IfT) for the aerosol layer above Leipzig

	UPM algorithm	IfT algorithm
Effective radius [μm]	0.15 ± 0.02	0.15 ± 0.01
Surface concentration [μm^2 cm^{-3}]	38.5 ± 5.4	49.8 ± 8.6
Volume concentration [μm^2 cm^{-3}]	1.85 ± 0.1	2.5 ± 0.6
Particle concentration [cm^{-3}]	573 ± 283	237 ± 61
Refraction index	1.56 ± 0.03	1.4 ± 0.05
	$0.0088i \pm 0.007$	$0.004i \pm 0.004$
Single scattering albedo (for 532 nm)	0.95 ± 0.35	0.97 ± 0.03

from the lidar measurements at the Leipzig station. The inversion results are given in Table 2. The UPM method is a hybrid regularization technique that is designed to work with different kind and number of optical data. For example, experimental data obtained with different systems at various wavelengths can be evaluated. Even bimodal and multimodal distributions can be retrieved without any knowledge of the number of modes in advance. The first regularization step is performed via projection discretization, in which the investigated distribution function is approximated with variable B spline functions. In a second step, regularization is controlled by the level of truncated singular-value decomposition performed during the solution process of the resulting linear equation system. For more details, see Böckmann and Sarközi (1999) and Böckmann (2001). Both inversion schemes showed an excellent agreement for an effective particle radius of 0.15 ± 0.02 μm, respectively. The volume concentration of 1.85 ± 0.1 as well as the surface-area concentration of 38.5 ± 5.4, respectively, are in a very good agreement to the results of the IfT. The algorithms found reasonable values even for the particle number concentration, which in general is difficult to determine, if a large number of small and thus optically less active particles are present. This fact was observed in the simulation retrievals. Whereas the size and concentration parameters were in good agreement, the algorithms showed discrepancies in the determination of the refractive index. The UPM algorithm computed a larger real part of 1.56 ± 0.03 as well as a comparably large imaginary part of 0.0088 ± 0.007. This finding is supported by the results from the ECMWF and NCEP trajectories, and is in better agreement with the high lidar ratios. The imaginary part is consistent with the observations of industrial-pollution particles (Wandinger et al., in press; Müller et al., in press; Böckmann, 2001).

4. Summary and conclusions

We have used lidar stations in the German Lidar Network to examine a post-colt-frontal air mass in January 2000. After the cold front passage, and while the air mass travelled from northern to southern Germany, the aerosol backscatter coefficient (β_{aer}) increased in the lower troposphere, but there was no change in the free troposphere. Trajectory models show that the observed air mass was lifted from the surface 2–3 days before it reached the lidar stations in Germany. Sinking of the air mass in the free troposphere released particles from evaporating cloud particles. Favourable conditions for these processes to act exist in high-pressure areas. The altitude of the temperature inversion is the principle lower boundary of the observed aerosol layer in the free troposphere. The trajectory analysis could not uniquely identify the location of the lifting process and hence the source of the aerosol layer. This case study suggests that after a cold front, the lifetime of an aerosol layer can be as long as a few days.

The aerosol backscatter coefficients from the aerosol layer above Kühlungsborn were compared with typical aerosol components in the Global Aerosol Data Set (GADS). This indicated that the aerosol layer above Kühlungsborn consisted of small particles. For the aerosol layer above Leipzig, inversion schemes were used, which showed continental aerosol of about 150 nm effective particle size.

Acknowledgements

We thank J. Bösenberg for coordinating with the German Lidar Network. This work was funded by the German Federal Ministry for Education, Science, Research and Technology (BMBF) within the Aerosol Research Program (AFS), contract no. 07AF113/0.

References

Ackermann, J., 1998. The extinction-to-backscatter ratio of tropospheric aerosol: a numerical study. J. Atmos. Oceanol. Technol. 15, 1043–1050.

Alpers, M., Eixmann, R., Höffner, J., Köpnick, T., Schneider, J., von Zahn, U., 1999. The Rayleigh/Mie/Raman lidar at IAP Kühlungsborn. J. Aerosol Sci. 30 (Suppl. 1), 637–638.

Althausen, D., Müller, D., Ansmann, A., Wandinger, U., Hube, H., Clauder, E., Zörner, S., 2000. Scanning six-wavelength eleven-channel aerosol lidar. J. Atmos. Oceanol. Technol. 17, 1469–1482.

Ansmann, A., Riebesell, M., Weitkamp, C., 1990. Measurement of atmospheric aerosol extinction profiles with a Raman Lidar. Technical Report 90/E/27, GKSS.

Ansmann, A., Wagner, F., Althausen, D., Müller, D., Herber, A., Wandinger, U., 2001. European pollution outbreaks during ACE~2: lofted aerosol plumes observed with Raman lidar at the Portuguese coast. J. Geophys. Res. 106 (D18), 20725–20734.

Böckmann, C., 2001. Hybrid regularization method for ill-posed inversion of multi-wavelength lidar data to retrieve aerosol size distribution. Appl. Opt. 40, 1329–1342.

Böckmann, C., Sarközi, J., 1999. The ill-posed inversion of multiwavelength lidar data by a hybrid method of variable projection. Proc. SPIE-Int. Soc. Opt. Eng. 312, 282–293.

Bösenberg, J., Böckmann, C., Eixmann, R., Matthias, V., Mattis, I., Trickl, T., Weigner, M., 1998. A lidar network for the establishment of an aerosol climatology. Proceedings of the 19th International Laser Radar Conference, Annapolis, pp. 23–24.

Bösenberg, J., Alpers, M., Althausen, D., Ansmann, A., Böckmann, C., Eixmann, R., Franke, A., Freudenthaler, V., Giehl, H., Jäger, H., Kreipl, S., Linne, H., Matthias, V., Mattis, I., Müller, D., Sarközi, J., Schneidenbach, L., Schneider, J., Trickl, T., Vorobieva, E., Wandinger, U., Wiegner, M., 2001. The German Aerosol Lidar Network, Methodology, Data Analysis, Max-Planck-Institut für Meteorologie Report No. 317, pp. 1–155.

Craven, P., Wahba, G., 1979. Smoothing noisy data with spline functions: estimating the correct degree of smoothing by the method of generalized cross-validation. Numer. Math. 31, 377–403.

d'Almeida, G.A., Köppke, P., Shettle, E.P. (Eds.), 1991. Atmospheric Aerosols, Global Climatology and Radiative Characteristics. A. Deepak Publishing, Hampton, 561 pp.

Fernald, F.G., 1984. Analysis of atmospheric lidar observations: some comments. Appl. Opt. 23, 652–653.

Golub, G.H., Heath, M., Wahba, G., 1979. Generalized cross-validation as a method for choosing a good ridge parameter. Technometrics 21, 215–223.

Hess, M., Koepke, P., Schult, I., 1998. Optical properties of aerosols and clouds: the software package OPAC. Bull. Am. Meteorol. Soc. 79, 831–844.

HYSPLIT4 (HYbrid Single-Particle Lagrangian Integrated Trajectory) Model, 1997. Web address: http://www.arl.noaa.gov/ready/hysplit4.html, NOAA Air Resources Laboratory, Silver Spring, MD.

Klett, J.D., 1985. Lidar inversion with variable backscatter/extinction ratios. Appl. Opt. 24, 1638–1643.

Kottmeier, C., Fay, B., 1998. Trajectories in the Antarctic lower troposphere. J. Geophys. Res. 105 (D9), 10947–10959.

Müller, D., Wandinger, U., Ansmann, A., 1999a. Microphysical particle parameters from extinction and backscatter lidar data by inversion with regularization: theory. Appl. Opt. 38, 2346–2357.

Müller, D., Wandinger, U., Ansmann, A., 1999b. Microphysical particle parameters from extinction and backscatter lidar data by inversion with regularization: simulation. Appl. Opt. 38, 2358–2368.

Müller, D., Wandinger, U., Althausen, D., 2001. Comprehensive particle characterization from 3-wavelength Raman-lidar observations: case study. Appl. Opt. 40, 4863–4869.

Russel, P.B., Hobbs, P.V., Stowe, L.S., 1999. Aerosol properties and radiative effects in the United States East

Coast haze plume: an overview of the Tropospheric Aerosol Radiative Forcing Observational Experiment (TARFOX). J. Geophys. Res. 104, 2213–2222.

Shettle, E.P., Fenn, R.W., 1976. Models of the atmospheric aerosols and their optical properties. Optical Properties in the Atmosphere, AGARD Conference Proceedings, N. 183, AGARD-CP-183.

Stohl, A., 1998. Computation, accuracy and applications of trajectories—a review and bibliography. Atmos. Environ. 32, 947–966.

Stohl, A., Wotawa, G., Seibert, P., Kromp-Kolb, H., 1995. Interpolation errors in wind fields as a function of spatial and temporal resolution and their impact on different types of kinematic trajectories. J. Appl. Meteorol. 34, 2149–2165.

Tikhonov, A.N., Arsenin, V.Y. (Eds.), 1977. Solution of Ill-Posed Problems. Wiley, New York, 258 pp.

United States Committee on Extension to the Standard Atmosphere, 1976. U.S. Standard Atmosphere, 1976. National Oceanic and Atmospheric Administration, Washington.

Wandinger, U., Müller, D., Böckmann, C., Althausen, D., Matthias, V., Bösenberg, J., Weiß, V., Fiebig, M., Wendisch, M., Stohl, A., Ansmann, A., 2001. Optical and microphysical characterization of biomass-burning and industrial-pollution aerosols from multiwavelength lidar and aircraft measurements. J. Geophys. Res., in press.